OXFORD

Cerebral Cortex, July 2016;26: 3036–3051

doi: 10.1093/cercor/bhv122
Advance Access Publication Date: 17 June 2015
Original Article

ORIGINAL ARTICLE

Cortical Effects on Ipsilateral Hindlimb Muscles Revealed with Stimulus-Triggered Averaging of EMG Activity

William G. Messamore[1], Gustaf M. Van Acker III[1], Heather M. Hudson[1], Hongyu Y. Zhang[1], Anthony Kovac[2], Jules Nazzaro[3] and Paul D. Cheney[1]

[1]Department of Molecular and Integrative Physiology, [2]Department of Anesthesiology and [3]Department of Neurosurgery, University of Kansas Medical Center, Kansas City, KS 66160, USA

Address correspondence to Paul D. Cheney, Department of Molecular and Integrative Physiology, University of Kansas Medical Center, 3901 Rainbow Blvd., Kansas City, KS 66160-7336, USA. Email: pcheney@kumc.edu

Abstract

While a large body of evidence supports the view that ipsilateral motor cortex may make an important contribution to normal movements and to recovery of function following cortical injury (Chollet et al. 1991; Fisher 1992; Caramia et al. 2000; Feydy et al. 2002), relatively little is known about the properties of output from motor cortex to ipsilateral muscles. Our aim in this study was to characterize the organization of output effects on hindlimb muscles from ipsilateral motor cortex using stimulus-triggered averaging of EMG activity. Stimulus-triggered averages of EMG activity were computed from microstimuli applied at 60–120 μA to sites in both contralateral and ipsilateral M1 of macaque monkeys during the performance of a hindlimb push–pull task. Although the poststimulus effects (PStEs) from ipsilateral M1 were fewer in number and substantially weaker, clear and consistent effects were obtained at an intensity of 120 μA. The mean onset latency of ipsilateral poststimulus facilitation was longer than contralateral effects by an average of 0.7 ms. However, the shortest latency effects in ipsilateral muscles were as short as the shortest latency effects in the corresponding contralateral muscles suggesting a minimal synaptic linkage that is equally direct in both cases.

Key words: EMG, hindlimb, ipsilateral, motor cortex, stimulus-triggered average

Introduction

While the actions of primary motor cortex on contralateral muscles and movements are well documented, the actions on ipsilateral muscles and the possible neural pathways mediating these actions are less clear. In addition to cortico-bulbar projections, the ipsilateral corticospinal track is a potential important pathway for cortical actions on ipsilateral motoneurons. It is well known that ~10% of corticospinal axons descend uncrossed in the spinal cord and many of these terminate ipsilaterally (Hutchins et al. 1988; Dum and Strick 1996; Lacroix et al. 2004; Jankowska and Edgley 2006). A relatively large body of evidence supports the view that ipsilateral corticospinal projections may make important contributions to normal movement and to recovery of function following unilateral cortical injury (Chollet et al. 1991; Fisher 1992; Caramia et al. 2000; Feydy et al. 2002). Unit recording studies have demonstrated that ~10% of neurons are modulated exclusively with ipsilateral limb movements (Matsunami and Hamada 1978; Tanji et al. 1988; Aizawa et al. 1990) and functional magnetic resonance imaging studies consistently show bilateral activation of motor cortex with unilateral limb movements (Cramer et al. 1999; Curt et al. 2002; Verstynen et al. 2005; Chiou et al. 2013). There is also evidence from animal studies supporting a contribution of ipsilateral corticospinal pathways to motor recovery following damage to contralateral motor cortex (Benecke et al. 1991; Chollet et al. 1991; Fisher

1992; Brus-Ramer et al. 2007; Gharbawie et al. 2007). Also, not to be overlooked are the projections from cerebral cortex to brainstem reticulospinal nuclei which have the potential to produce robust actions on ipsilateral motoneurons at both cervical and lumbar levels of the spinal cord (He and Wu 1985; Keizer and Kuypers 1989; Davidson and Buford 2004; Davidson et al. 2007; Riddle et al. 2009).

Although there are numerous studies supporting a role of ipsilateral cortex in the control of both proximal and distal limb movements, the contribution of ipsilateral cortex to movement in the absence of CNS damage remains controversial. For example, Soteropoulos et al. (2011) failed to find any significant synaptic linkage from the ipsilateral corticospinal tract to hand and forearm motoneurons using intracellular recording, stimulus-triggered averaging of EMG activity or spike-triggered averaging of EMG activity in macaque monkeys. In human subjects recovering from stroke, Palmer et al. (1992) used TMS to elicit changes in the firing probability of biceps motor units and failed to detect any short latency synaptic linkage with ipsilateral motoneurons.

The position of the M1 hindlimb representation in primates on the midline of the hemisphere provides optimal access to both ipsilateral and contralateral M1 through a single recording chamber and presents an ideal opportunity to collect definitive data on the properties (sign, strength, latency, and muscle distribution) of the ipsilateral corticospinal projection using stimulus-triggered averaging of EMG activity in awake monkeys (Cheney and Fetz 1985; Cheney et al. 1985; Kasser and Cheney 1985; Park et al. 2001; Boudrias et al. 2006; Griffin et al. 2009; Hudson et al. 2015). The goal of this study was to extend our previous work characterizing cortical output to contralateral hindlimb muscles (Hudson et al. 2013, 2015) by quantifying the output properties from ipsilateral hindlimb M1 cortex relative to contralateral M1 in terms of magnitude, latency, and distribution of effects on hip, knee, ankle, digit, and intrinsic foot muscles.

Experimental Procedures

All work involving monkeys conformed to the procedures outlined in the Guide for the Care and Use of Laboratory Animals published by the US Department of Health and Human Services and the National Institutes of Health. All animal procedures were approved by the Institutional Animal Care and Use Committee.

Behavioral Task

Two male rhesus macaques (*Macaca mulatta*) were trained to perform a hindlimb push–pull task as described previously (Hudson et al. 2010). Inside a sound-attenuated chamber, the monkey was seated in a custom-built primate chair facing a computer monitor providing visual and auditory feedback. Both of the monkey's forelimbs were comfortably restrained, as well as the monkey's left hindlimb, while the task was performed with the right hindlimb. The task consisted of the monkey grasping a horizontal post with the foot of its right hindlimb. The monkey performed push–pull movements with the leg alternating between targets in flexion and extension. Movements away from a central starting position, with the knee at ~90°, were opposed by an elastic load. Successful performance required holding in each target zone for 750 ms at which point a food reward was delivered to the monkey's mouth. The task was designed to produce broad activation of both proximal and distal hindlimb muscles making it an ideal model in which to investigate the output properties of contralateral and ipsilateral motor cortex using stimulus-triggered averaging of EMG activity.

Surgical Procedures

As a prophylactic measure against infection, injectable liquid penicillin (6000 U/kg) was given on the day before surgery, the day after surgery, and at 3 days after surgery. The monkeys were tranquilized with ketamine (10 mg/kg) for transport and anesthetized with isoflurane gas. Atropine (0.04 mg/kg) was given to reduce secretions and prevent bradycardia. The monkey's forelimb, neck, back, hip, hindlimb and foot were shaved and sterilized (Betadine: 10% povidone-iodine). Temperature, blood pressure, EKG, and blood oxygenation were monitored. Following surgery, the monkey was closely monitored until it was fully awake and able to sit and stand without assistance. Post-operative analgesics (buprenorphine, 0.01 mg/kg) were given for 3 days. Wound edges around the cortical chamber were inspected daily and treated with topical antibiotic.

Cortical Chamber Implant

Magnetic resonance imaging (MRI) was done on each monkey to determine the optimal placement for the cortical chamber based on the monkey's cortical anatomy (Fig. 3). Using the intersection of the central sulcus and sagittal sinus as a general anatomical landmark, the chambers were centered over the midline and positioned stereotaxically at anterior 14.5 mm (Snider and Lee 1961). This location provided access to the hindlimb representation of M1 in both hemispheres. A 30-mm-diameter craniotomy was performed, and a titanium recording chamber was attached to the skull using dental acrylic held in place with 12 titanium skull screws (Stryker, Inc.). Titanium nuts for anchoring a restraining head bar were also attached at this time over the occipital skull with dental acrylic and an additional 12 titanium screws. The head bar provided a flexible restraint to limit head movements during cortical recordings.

An alternative approach to this experiment would have been to record simultaneously from both the left and right legs while stimulating sites in the cortex. While this approach would have had the advantage eliminating cortical site variability, it would have had the disadvantage of EMG implant variability. For this and other practical reasons, we chose the alternative approach of stimulating the 2 hemispheres separately while recording from muscles of only one hindlimb.

Based on criteria established by others (Mitz and Wise 1987; Luppino et al. 1991), we are confident that all our stimulus sites were in M1 and none were in supplementary motor cortex (SMA). The posterior border of SMA is located approximately 7 mm posterior to the posterior limit of the arcuate sulcus. The most anterior points from which we obtained poststimulus effects (PStEs) were all posterior to this boundary (Fig. 3). Also, supporting the conclusion that all stimulus sites were in M1 is the fact that the representation of the hindlimb in SMA is very limited based on mapping studies using short train ICMS to evoke movements and what does exist tends to be in the medial wall of the hemisphere (Macpherson et al. 1982; Mitz and Wise 1987). In contrast, most of the hindlimb representation from M1 we found was on the dorsal surface rather than the medial wall of the hemisphere.

EMG Modular Subcutaneous Implant

We used the modular arm-mounted subcutaneous implant method described by Hudson et al. (2010, 2015) in which EMG connectors are attached to the upper arm and the wires tunneled to an incision on the back and then to muscles of the hindlimb. Two small incisions (5 mm) were made approximately half way

between the shoulder and the elbow on the lateral surface of the proximal forelimb. These incisions were the entry points for the wires running subcutaneously to the hindlimb. A vertical incision (~4 cm) was made on the back near the midpoint between the scapulae. This incision functioned first as a turning point for the subcutaneous tunneling of the wires from the forelimb to the hindlimb, and second, as a final anchoring point for the wires. Custom designed needles fabricated from stainless steel rods were used to tunnel the EMG wires. Each needle had a pointed tip with a non-cutting edge. The opposite end was flattened with 3–5 eyes. The wires were threaded through the eyes and folded back for tunneling under the skin. Bundles of wires were tunneled subcutaneously through the incisions on the forelimb to the incision on the back and then on to the individual target muscles.

The modular implant uses single-layer connector modules (ITT, Cannon) that can be affixed to the skin as described by Park et al. (2000). Forty-four multi-stranded stainless steel wires were cut to lengths appropriate for the 22 pairs of EMG wires to be implanted. Twenty-two muscles were selected for implantation. These muscles spanned 3 joints and were a mix of abductors, adductors, flexors, and extensors. The wires were divided into 4 modules based on the location of the muscles to be implanted: proximal-lateral (gluteus maximus—GMAX, semimembranosus—SEM, gracilis—GRA, long head of biceps femoris—BFL, semitendinosus—SET); proximal-medial (adductor brevis—ADB, vastus medialis—VM, sartorius—SAR, rectus femoris–RF, tensor facia lata–TFL, vastus lateralis—VL); distal-lateral (extensor digitorum brevis—EDB, extensor digitorum longus–EDL, peroneus longus–PERL, distal portion of soleus—SOLd, proximal portion of soleus—SOLp, lateral gastrocnemius—LG); and distal-medial (medial gastrocnemius—MG, flexor digitorum longus—FDL, flexor hallucis brevis—FHB, tibialis anterior—TA, abductor hallucis—AH). The actions of these muscles are summarized in Hudson et al. (2010). Connectors were constructed as described by Park et al. (2000), and the wires were color coded to make identification and implantation more efficient.

After tunneling, each wire was cut to length, leaving 6–7 cm exteriorized at the target muscle site. For each wire, 2–3 mm of insulation was removed from the tip. Each wire was back-fed into a 22-gauge hypodermic needle and folded back along the shaft of the needle. The wire was then inserted into the muscle in a proximal direction through the same puncture incision in the skin used for tunneling. The wire was held at its entry point into the skin, and the needle was removed leaving the EMG wire with a hooked tip anchored in the muscle belly. Two wires were inserted in each muscle with a target separation of ~5 mm. Electrical stimulation through the electrode pair was used to confirm proper placement as described previously by Hudson et al. (2010). A loop of wire remained exteriorized until confirmation of proper placement in the target muscle. The wires were then pulled centrally from the opening on the back until the loop disappeared under the skin without kinking.

Recording

EMG activity, cortical neural activity, and task-related signals were all monitored using Cambridge Electronic Design Spike2 software running custom scripts developed for our laboratory (Spike2 Neural Averager). EMGs and task-related activity were digitized at a rate of 8 kHz; cortical neural activity and the stimulus current monitor signal were digitized at a rate of 16 kHz. A manual hydraulic microdrive attached to the cortical chamber was used to lower glass-insulated platinum-iridium electrodes into layer V of M1 in the hindlimb representation. The Spike2 data provided a continuous recording across all channels of each day's recording session. This data could be used to monitor signals on-line to confirm the quality of the EMG recordings and also offline for computation of stimulus-triggered averages. Stimulus-triggered averages of EMG activity were additionally computed on-line using custom Windows Averager software (Larry Shupe). For stimulus-triggered averages, microstimuli (30, 60, and 120 μA at 5 Hz, and twin pulses of 120 μA separated by 3 ms at 5 Hz) were applied through the microelectrode. Averages were obtained for all 22 implanted muscles over a 200-ms epoch, including 40 ms before the trigger to 160 ms after the trigger and a minimum of 2000 trigger events. Evaluation of poststimulus facilitation (PStF) and poststimulus suppression (PStS) was done using both the Windows Averager Software and Spike2 Neural Averager software.

Results

Data Summary and Location of Electrode Tracks

Microstimuli ranging in intensity from 30 to 120 μA revealed both excitatory and inhibitory effects in contralateral hindlimb muscle EMG activity as illustrated in Figure 1. Significant PStF effects were conservatively identified as transient increases in EMG activity in which the mean-to-noise ratio of peak points was ≥2.25. Mean-to-noise ratio is defined as the difference between the baseline mean and the mean of points in the peak, divided by the baseline standard deviation. In other words, it expresses the mean PStF increase over baseline in units of standard deviation. The onset and termination of PStF were identified as points where the envelope of the effect crossed a line representing 2 standard deviations of the baseline mean. These criteria are illustrated in Figure 1. Analogous criteria were applied to the identification of PStS.

PStF was interpreted as evidence of an underlying excitatory synaptic linkage between the population of stimulated cells and the target motoneurons. PStS was interpreted as evidence of an underlying inhibitory synaptic linkage between the population of stimulated cells and the target motoneurons. Stimulus-triggered averages showing no poststimulus change in average EMG activity were interpreted as evidence that the stimulated neurons lacked a synaptic linkage with motoneurons.

Figure 2 shows poststimulus effects from ipsilateral cortex and contralateral cortex at stimulus intensities of 30, 60, and 120 μA using standard stimulus-triggered averaging procedures. In an effort to compensate for the effects of a weaker synaptic linkage, we also computed averages from twin-pulse stimulation (3 ms inter-stimulus interval, 5 Hz repetition rate) at 120 μA. Early PStF and PStS are clear at 30 μA in contralateral muscles (VM, SAR, FDL). A late, broad suppression is also evident (EDB, VL). These effects become stronger at 60 μA, and now a short latency PStS also appears in VL. At 120 μA, short latency PStF and PStS become very prominent along with a broad, late suppression. Effects in the same muscles from an ipsilateral cortical site (Fig. 2, upper panel) were much weaker, although clearly present at the higher intensities. The cortical site illustrated in Figure 2 was typical in showing a complete absence of ipsilateral effects at 30 μA. At 60 μA, very weak effects were present in FDL and SOLd. These effects became clearer and much stronger at 120 μA and additional effects appeared in all the other muscles illustrated. As expected, application of twin pulses further strengthened the effects.

The nature (facilitation/suppression) and appearance of both the contralateral and ipsilateral effects remained relatively

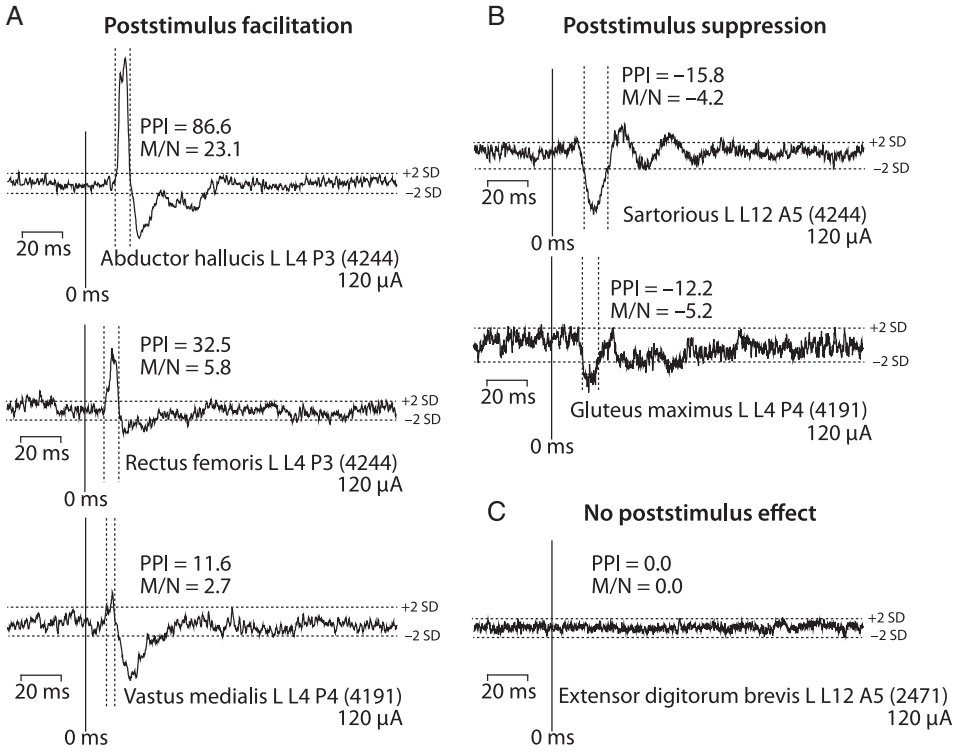

Figure 1. Types of poststimulus effects observed in stimulus-triggered averages of EMG activity at 120 µA applied to the contralateral hemisphere. (A) Poststimulus facilitation (PStF) is a transient increase in firing probability of motor units revealing an excitatory linkage between the population of cells stimulated and target motoneurons. (B) Poststimulus suppression (PStS) is a transient decrease in firing probability indicating an inhibitory linkage between the population of cells stimulated and target motoneurons. (C) Effects that showed no increase or decrease in firing probability indicating no synaptic linkage. The numbers in parenthesis indicate the number of stimulus trigger events on which the average is based. PStF and PStS were quantified both as the percent peak increase above baseline (PPI) and the mean-to-noise ratio (M/N) of the effect (see text). The onset and termination of PStF and PStS effects were defined as the points where the record crossed lines representing 2 standard deviations of the pre-trigger baseline average (horizontal dotted lines). The vertical dotted lines illustrate for strong and weak PStF effects the portion of the record that was counted as a significant effect.

constant at all intensities and with application of twin pulses. For example, the contralateral VL muscle showed early and late PStS at 60 µA, and these effects remained intact even with twin pulses at 120 µA. Although effects were present at lower intensities, to facilitate comparison of ipsilateral and contralateral effects, we chose 120 µA (single pulse) as the standard stimulus intensity to apply at all cortical sites.

Table 1 summarizes the data collected from contralateral and ipsilateral M1 in 2 male rhesus macaques. Data were obtained from a total of 679 electrode tracks (Monkey M, 337; Monkey L, 342; location shown in Fig. 3). Stimulus-triggered averages were collected from 22 muscles of the hip, knee, ankle, digit, and intrinsic foot for a total of 20 416 average records. Muscles with poor EMG signal or artifact were eliminated, leaving 18 muscles for comparison. Because of the importance of soleus as a slow muscle, 2 pairs of electrodes were used with 1 pair placed proximally and a second pair distally in the muscle. The total number of independent muscles tested was therefore 17. At 57 sites, high-frequency, short-duration intracortical microstimulation (ICMS, 13 pulse train at 333 Hz, 120 µA) was used to test for motor output effects outside the hindlimb representation including trunk, shoulder, and tail movements. Neurons at an additional 67 sites had sensory responses aiding in the detection of the border of primary somatosensory cortex. Of 20 416 averages, 6866 showed some poststimulus effect, 5414 of which were PStFs and 1452 of which were PStSs. Only stimulus-triggered averages (StTAs) where the earliest effect was suppression were counted as PStS effects.

Distribution of PStF across Muscles of Different Joints

The number of PStF effects sorted by joint and muscle is given in Figure 4. An effect was included as PStF if facilitation was the earliest effect, although many PStE effects were biphasic with facilitation followed by suppression (for example, AH and VM in Fig. 1). Summing results across all cortical sites tested at 120 µA, ipsilateral PStF was observed in every muscle across all joints. The same was true of PStS. As with contralateral effects, ipsilateral PStF (Fig. 4, right side) was much more prevalent than ipsilateral PStS (Fig. 4, left side). Also noteworthy is the fact that some ipsilateral muscles, including at least 1 at each joint, had 2–3 times as many PStF effects as other muscles at the same joint. These muscles were MG at the ankle, VM, and SAR at the knee and GMAX at the hip. Interestingly, the same contralateral muscles also showed the most effects, although the differences were not near as dramatic as for the ipsilateral muscles. A similar result exists for PStS. The contralateral muscle showing the greatest number of PStS effects was ADB (hip), and ADB also showed the greatest number of effects among ipsilateral muscles both with single-pulse and twin-pulse stimulation.

Magnitude of Ipsilateral versus Contralateral PStF

Table 2 summarizes the average magnitudes of contralateral and ipsilateral effects in each monkey expressed as percent peak increase over baseline (PPI) for each muscle group with the corresponding average mean-to-noise ratio. The data for muscles at each joint (hip, knee, ankle, digit, and intrinsic foot) are

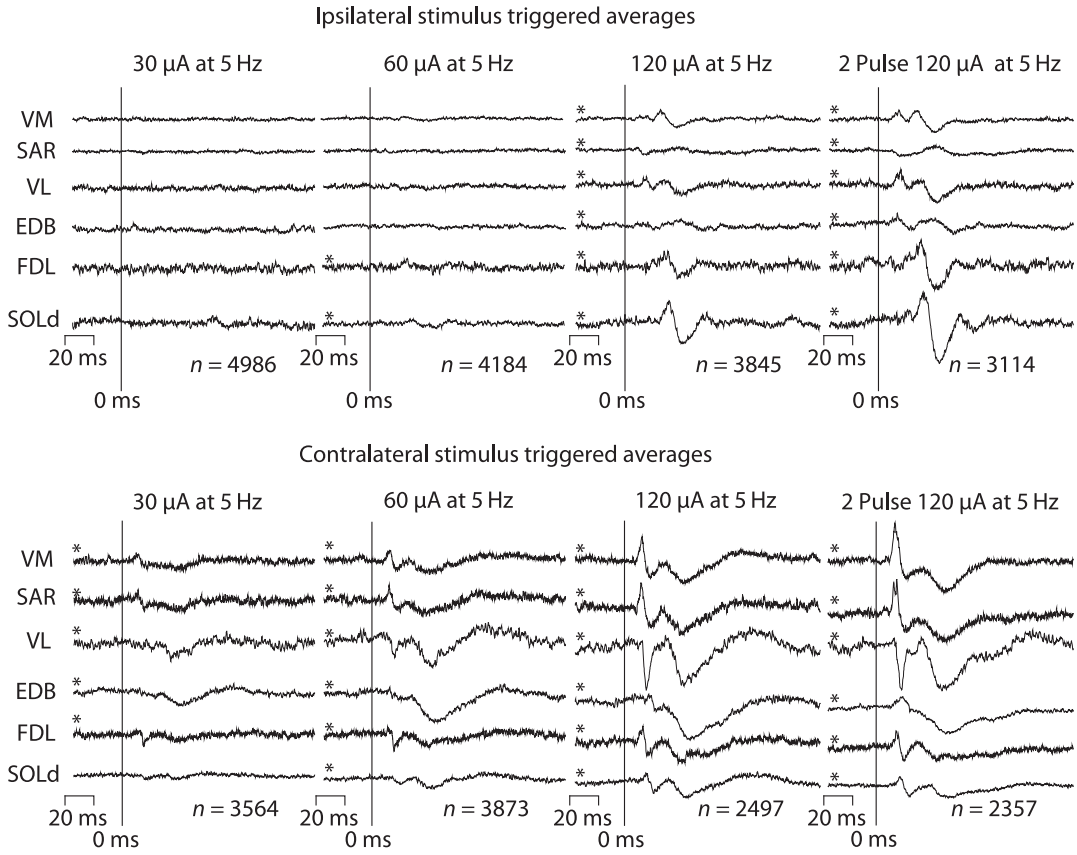

Figure 2. Stimulus-triggered averages of EMG activity using various stimulus currents of 30, 60, 120 μA and twin pulses at 120 μA (3 ms pulse separation). Stimuli were applied to ipsilateral and contralateral primary motor cortex in the same monkey. Effects from stimulation of the ipsilateral cortex at 30 μA are absent, and effects at 60 μA are too weak and too few in number for adequate comparison with contralateral effects. Stimulation of the ipsilateral cortex at 120 μA yielded clear and consistent effects that could be compared with contralateral effects in terms of sign, latency, and magnitude. Asterisks denote effects that met our inclusion criteria for PStF and PStS effects.

Table 1 Summary of data collected

	Monkey M			Monkey L			Total
Electrode tracks	337			342			679
RL-ICMS sites[a]	31			26			57
Sensory test	38			29			67
	Contralateral 120 μA	Ipsilateral 120 μA	Ipsilateral 2 pulse 120 μA	Contralateral 120 μA	Ipsilateral 120 μA	Ipsilateral 2 pulse 120 μA	
Sites stimulated	143	156	156	157	158	158	928
StTA records (all)	3146	3432	3432	3454	3476	3476	20 416
Sites yielding PStEs	143	152	156	155	158	158	922
Sites yielding PStF	143	151	156	155	158	158	921
Sites yielding PStS	125	91	106	110	106	132	670
PStEs obtained	1491	406	1001	2018	577	1373	6866
PStF effects	1156	361	808	1702	431	956	5414
PstS effects	335	45	193	316	146	417	1452

[a]13 pulse train at 333 Hz, 120 μA done for testing sites outside the hindlimb representation.

presented as well as the overall mean across all muscles. At the same stimulus intensity (120 μA), the average magnitude of contralateral facilitation effects was ~2–6 times greater than the corresponding ipsilateral effects (Monkey M, 25.7 vs. 10.6 PPI, $P < 0.000001$; Monkey L, 67.0 vs. 12.0 PPI, $P < 0.000001$) depending on the monkey and muscle group.

Monkey L's contralateral PStF was substantially stronger at each joint than contralateral PStF in monkey M. This was particularly true of distal muscles. Overall, contralateral PStF in Monkey L was 2.6 times greater than contralateral PStF in Monkey M. Ipsilateral PStF did not show similar differences. The mean ipsilateral PStF was similar (10.6 vs. 12.0, PPI) in the 2 monkeys.

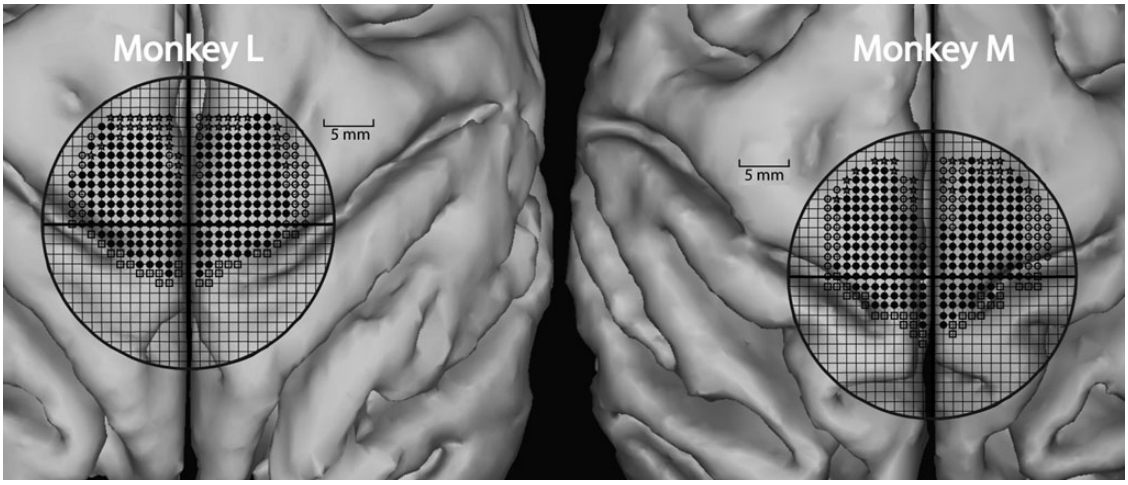

Figure 3. Contralateral and ipsilateral tracks in Monkey M and Monkey L. A 1 × 1 mm grid is superimposed onto a 3D reconstruction of MRIs for both monkeys. The dark circle outlines the interior circumference of the implanted cortical chamber. Solid circles represent electrode tracks that produced hindlimb movement with high-frequency, short-duration ICMS (13 pulses @ 330 Hz). Open circles represent electrode tracks that produced non-hindlimb responses (trunk, tail, etc.) with ICMS. Stars represent electrode tracks that did not produce visible movement with ICMS. Open boxes represent electrode tracks that were positive on sensory testing and helped identify the border of primary somatosensory cortex.

As expected, twin-pulse stimulation increased the magnitude of ipsilateral PStF. The average increase was 34% in Monkey L and 41% in Monkey M. There was no evidence for any significant variation in the magnitude of ipsilateral PStF for muscles at different joints. For contralateral effects, distal muscles (ankle, foot, and intrinsic foot) had significantly stronger PStF than proximal muscles.

PStS was also detectable ipsilaterally but was weaker than contralateral PStS. The average magnitude of contralateral PStS was nearly two-fold greater than ipsilateral PStS (Monkey M, −16.0 vs. −9.5 PPI, $P < 0.000001$; Monkey L, −18.8 vs. −10.2 PPI, $P < 0.000001$). Ipsilateral PStF was only slightly stronger than ipsilateral PStS: 1.1 times ipsilateral PStS in Monkey M and 1.2 times in Monkey L. For comparison, the magnitude of contralateral PStF was 1.6 times greater than contralateral PStS in Monkey M and 3.6 times greater in Monkey L. PStS was similar in strength in the 2 monkeys but PStF was much stronger in Monkey L compared with Monkey M.

Figure 5*A*,*B* shows histograms of the magnitude of PStF effects in ipsilateral and contralateral muscles at 120 μA separated by joint and also lumped together (All Muscles histograms). The differences in the distributions for contralateral and ipsilateral muscles are readily apparent for muscles at each joint. As a point of comparison, we used 20 peak percent increase (PPI) to separate the stronger from weaker effects. A little over half (54.1%) of the contralateral effects (Fig. 5*B*, All Muscles) were stronger than 20 PPI. In comparison, ipsilateral effects were much weaker with only 4.1% of effects greater than 20 PPI. Note the bar at 200+ PPI in the contralateral histograms. As mentioned previously, the magnitude of effects in Monkey L were considerably greater overall than those in Monkey M. Not surprisingly, most of the very strong effects (200 PPI and greater) came from Monkey L. Although the histograms for the contralateral muscles were skewed toward higher magnitudes, the peaks of the distributions for contralateral and ipsilateral muscles were surprisingly similar (12 PPI contralateral vs. 10 PPI ipsilateral, All Muscles, Fig. 5*B*).

Latency of Ipsilateral versus Contralateral PStF and PStS

Table 3 summarizes the mean onset latency of contralateral and ipsilateral poststimulus effects from M1 in both monkeys. The data for muscles at each joint (hip, knee, ankle, digit, and intrinsic foot) are presented as well as the overall means. In both monkeys, the mean onset latency of PStF in contralateral muscles in the same muscle group was the same or shorter than the mean ipsilateral onset latency. The only exception was the ankle where the mean latency was shorter in ipsilateral muscles by 0.5 ms in 1 monkey and 0.6 ms in the second monkey compared with contralateral muscles. The overall mean difference in latency was 0.1 ms for Monkey M and 1.9 ms for Monkey L. The range for different muscle groups was 0–4.4 ms for Monkey M and 0.5–11.9 ms for Monkey L, all longer in ipsilateral muscles except for ankle muscles as noted above. The greater latency disparity for Monkey L correlates with this monkey's overall greater magnitude of PStF compared with Monkey M.

The results were more variable for PStS. In some cases, the mean latency was shorter for contralateral PStS, and in other cases, it was shorter for ipsilateral PStS. The overall mean latency for contralateral PStS was 20.2 ms in Monkey M and 16.7 ms for Monkey L compared with ipsilateral PStS onset latencies of 19.8 ms for Monkey M and 17.4 ms for Monkey L.

An important question regarding the latency of effects is whether the shortest latency effect ipsilaterally is as short as the shortest contralateral latency. Figure 6*A*,*B* shows histograms of the onset latencies of ipsilateral and contralateral PStF for each monkey and all muscles separated by joint, as well as the overall totals (120 μA). Longer latency PStF effects were more common for sites in ipsilateral cortex compared with contralateral cortex. For example, 18.6% and 6.9% of ipsilateral effects had latencies over 20 ms compared with only 1.6% and 1.8% contralaterally for Monkeys L and M, respectively. However, surprisingly the shortest onset latencies for effects from the contralateral and ipsilateral cortices were nearly the same for some muscle groups in each monkey. In Monkey M, the shortest onset latencies for contralateral compared with ipsilateral effects were within 0.1 ms of each other (Fig. 6*B*, All Muscles, Range). In Monkey L, the difference was 0.4 ms. Looking at individual muscle groups, in Monkey M the shortest latency effect in contralateral compared with ipsilateral muscle groups for the hip, knee, and ankle was either the same or different by only 0.1 ms. In Monkey L, the difference was 0.2 ms for hip muscles, 0.7 ms for knee muscles, and 0.4 ms for ankle

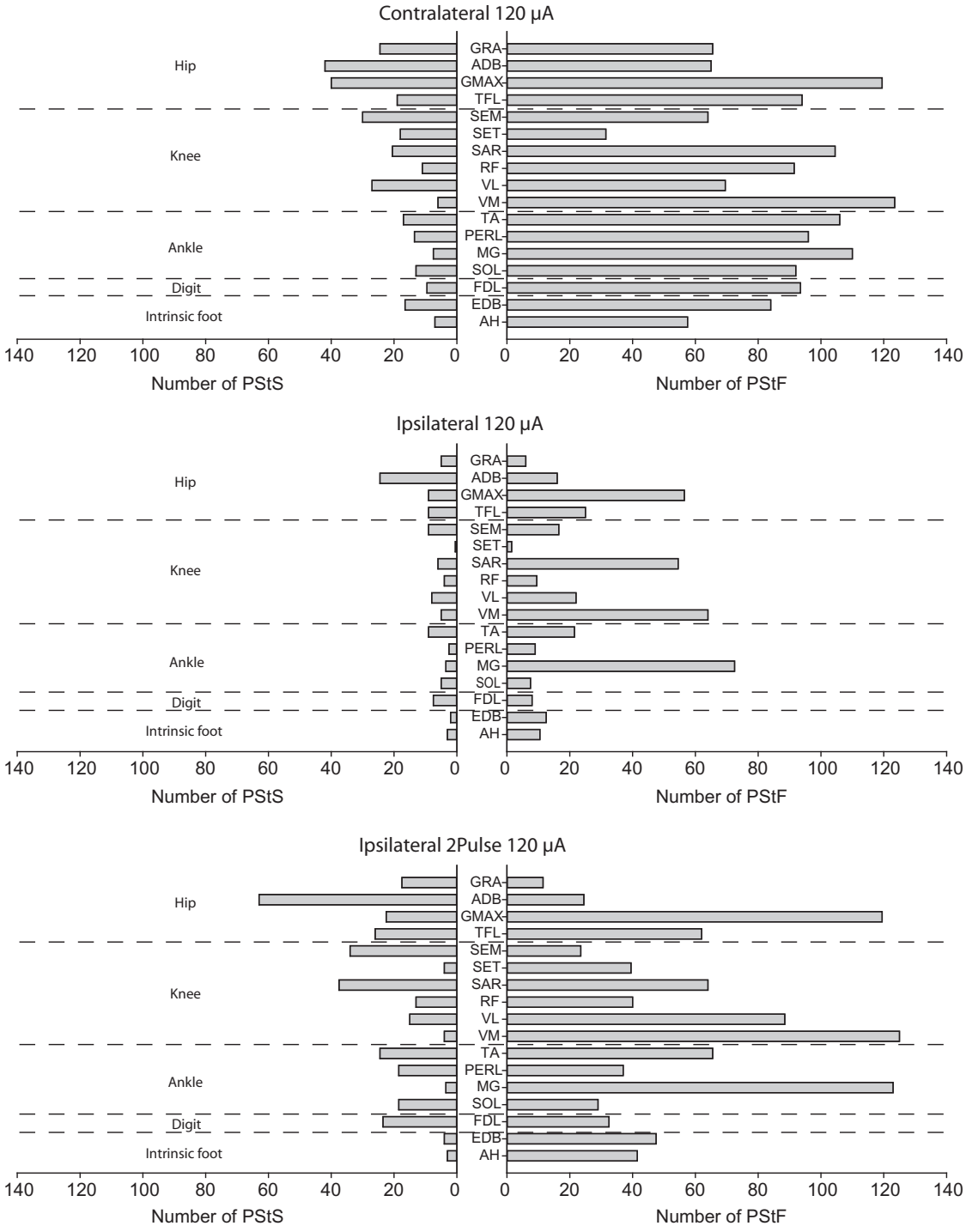

Figure 4. Number of contralateral and ipsilateral PStF and PStS effects at 120 μA in each hindlimb muscle listed by joint averaged across Monkeys M and L. For comparison, results are also presented for twin-pulse stimulation at 120 μA (3-ms interval) in the ipsilateral hemisphere.

muscles with contralateral effects being shorter in each case. Overall, in 5 of 6 comparisons (3 muscles groups in each of 2 monkeys), the shortest latency effect in ipsilateral muscles was either the same or within 0.4 ms of the shortest latency contralateral effect in the same muscle group. The number of effects in ipsilateral distal and intrinsic foot muscles was too small to be confident of the shortest latency effect with the possible exception of the intrinsic foot muscles in Monkey L where there were 33 ipsilateral effects. In this case, the shortest latency ipsilateral effect was 0.7 ms longer than the shortest latency contralateral effect.

The overall mean of the shortest onset latencies across contralateral hip, knee, ankle, and intrinsic foot muscle groups in Monkey L was 7.1 ms compared with 7.65 ms for ipsilateral muscle groups ($P = 0.745$); in Monkey M (hip, knee, and ankle muscles), they were identical at 7.93 ms ($P = 0.918$). The mean onset latency of ipsilateral effects for all muscle groups was appreciably greater than the mean of contralateral effects in all

Table 2 Comparison of magnitudes from contralateral and ipsilateral cortices

	Contralateral 120 μA			Ipsilateral 120 μA			Ipsi 2 pulse 120 μA		
Joint	*n*	PPI	M/N	*n*	PPI	M/N	*n*	PPI	M/N
Monkey M									
PStF									
Hip	173	15.9 ± 13.0	5 ± 4.1	34	9.4 ± 2.3	2.8 ± 0.5	86	14.5 ± 9.0	4.5 ± 2.2
Knee	481	23.5 ± 18.0	6.7 ± 4.8	220	11.3 ± 4.4	3.6 ± 1.2	411	16.9 ± 9.0	5.1 ± 2.4
Ankle	346	32.8 ± 28.9	8.5 ± 7.0	89	9.4 ± 2.5	2.8 ± 0.5	227	12.3 ± 4.4	3.9 ± 1.2
Digit	80	21.7 ± 14.7	6 ± 4.2	7	9.5 ± 2.2	2.6 ± 0.3	40	9.8 ± 3.0	3.0 ± 0.7
Intrinsic	76	34.2 ± 46.1	7.8 ± 7.2	13	11.3 ± 2.5	2.9 ± 0.9	102	14.8 ± 8.6	5.3 ± 2.6
Total	1156	25.7 ± 24.6	7 ± 5.7	363	10.6 ± 3.9	3.3 ± 1.1	866	14.9 ± 8.1	4.7 ± 2.2
PStS									
Hip	86	−13.4 ± 5.6	−4.3 ± 2.1	8	−9.4 ± 2.3	−2.7 ± 0.3	51	−9.8 ± 3.7	−3.4 ± 0.9
Knee	137	−16.2 ± 6.1	−4.7 ± 1.9	23	−9.7 ± 3.0	−2.7 ± 0.6	67	−12.3 ± 4.3	−3.5 ± 1.2
Ankle	75	−17.5 ± 7.7	−5.7 ± 2.5	12	−9.5 ± 2.3	−2.7 ± 0.3	67	−11.9 ± 4.0	−3.5 ± 0.8
Digit	6	−14.4 ± 4.3	−5.0 ± 2.0	1	−9.8 ± 0.0	−2.5 ± 0.0	2	−8.6 ± 2.6	−2.6 ± 0.1
Intrinsic	31	−19.3 ± 8.4	−5.6 ± 2.8	1	−6.0 ± 0.0	−2.4 ± 0.0	7	−12.1 ± 3.2	−3.0 ± 0.8
Total	335	−16.0 ± 6.8	−4.9 ± 2.3	45	−9.5 ± 2.7	−2.7 ± 0.5	194	−11.5 ± 4.1	−3.4 ± 1.0
Monkey L									
PStF									
Hip	327	33.2 ± 31.5	7.3 ± 6.6	123	12.2 ± 6.2	3.1 ± 1.1	225	16.4 ± 13.5	4.0 ± 1.8
Knee	488	40.7 ± 38.5	9.2 ± 8.1	116	11.6 ± 4.7	3.1 ± 0.8	350	17.3 ± 12.6	4.5 ± 2.3
Ankle	573	95.1 ± 121.7	17.7 ± 19.3	150	12.5 ± 3.9	3.8 ± 1.2	222	16.1 ± 7.1	3.8 ± 1.5
Digit	107	96.8 ± 128.2	15.9 ± 17.5	9	9.8 ± 1.6	2.7 ± 0.3	25	11.4 ± 13.0	3.1 ± 0.7
Intrinsic	207	89.0 ± 133.3	17.7 ± 20.2	33	10.4 ± 3.1	2.9 ± 0.9	134	13.0 ± 16.1	3.9 ± 1.9
Total	1702	67.0 ± 98.0	13.1 ± 15.6	431	12.0 ± 4.8	3.3 ± 1.1	956	16.1 ± 10.6	4.1 ± 2.0
PStS									
Hip	142	−20.5 ± 9.0	−4.8 ± 2.4	65	−10.4 ± 2.6	−2.9 ± 0.5	155	−16.1 ± 6.3	−4.3 ± 1.8
Knee	99	−18.3 ± 7.6	−4.8 ± 2.5	36	−10.2 ± 2.4	−3.0 ± 0.6	148	−14.7 ± 5.8	−4.8 ± 2.1
Ankle	39	−15.5 ± 7.4	−3.8 ± 1.8	25	−10.3 ± 3.7	−2.8 ± 0.5	61	−11.2 ± 3.8	−3.4 ± 0.9
Digit	18	−23.3 ± 7.7	−4.7 ± 2.8	13	−10.2 ± 2.2	−2.8 ± 0.4	45	−12.6 ± 3.0	−3.7 ± 0.8
Intrinsic	18	−11.6 ± 4.9	−3.7 ± 1.2	7	−8.9 ± 1.1	−2.8 ± 0.3	8	−12.2 ± 2.4	−3.8 ± 0.9
Total	316	−18.8 ± 8.5	−4.6 ± 2.4	146	−10.2 ± 2.7	−2.9 ± 0.5	417	−14.4 ± 5.7	−4.3 ± 0.9
Total									
PStF									
Hip	500	27.2 ± 27.9	6.5 ± 2.3	157	11.6 ± 5.7	3.1 ± 1.0	311	15.9 ± 12.4	4.1 ± 1.9
Knee	969	32.2 ± 31.4	7.9 ± 6.8	336	11.4 ± 4.5	3.4 ± 1.1	761	17.1 ± 10.8	4.9 ± 2.4
Ankle	919	71.6 ± 102.3	14.2 ± 16.4	239	11.3 ± 3.7	3.4 ± 1.1	590	14.7 ± 6.5	4.4 ± 2.1
Digit	187	64.7 ± 104.3	11.7 ± 14.4	16	9.7 ± 1.9	2.7 ± 0.3	65	10.4 ± 3.1	3.0 ± 0.7
Intrinsic	283	74.3 ± 119.0	15.0 ± 18.2	46	10.7 ± 3.0	2.9 ± 0.9	178	13.5 ± 7.6	4.1 ± 2.3
Total	2858	50.3 ± 79.8	10.7 ± 12.9	794	11.3 ± 4.5	3.3 ± 1.1	1905	15.6 ± 9.7	4.5 ± 2.2
PStS									
Hip	213	−17.6 ± 8.5	−4.8 ± 2.3	77	−10.3 ± 2.6	−2.6 ± 1.3	206	−14.5 ± 6.4	−4.1 ± 1.7
Knee	225	−17.0 ± 6.8	−4.9 ± 2.1	66	−10.0 ± 2.6	−2.2 ± 2.5	215	−14.0 ± 5.5	−4.4 ± 2.0
Ankle	108	−16.9 ± 7.6	−5.2 ± 2.4	43	−10.0 ± 3.4	−2.1 ± 2.0	133	−11.6 ± 3.9	−3.4 ± 0.8
Digit	19	−20.5 ± 8.0	−5.6 ± 2.4	16	−10.2 ± 2.1	−2.4 ± 1.2	47	−12.4 ± 3.0	−3.6 ± 0.9
Intrinsic	47	−16.6 ± 8.2	−5.1 ± 2.5	11	−8.5 ± 1.4	−1.9 ± 1.4	14	−12.2 ± 2.8	−3.4 ± 0.9
Total	612	−17.3 ± 7.8	−5.0 ± 2.3	213	−10.1 ± 2.7	−2.3 ± 1.9	615	−13.5 ± 5.5	−4.0 ± 1.6

muscle groups except the ankle and knee muscles in Monkey M and the ankle muscles in Monkey L (Table 3).

Latency of Effects with Twin-pulse Stimulation

Figure 7 contains histograms of ipsilateral PStF onset latencies for a proximal muscle group (knee), a distal muscle group (intrinsic foot), as well as all muscles combined for twin-pulse stimulation at 120 μA. There is a clear bimodality in the histograms of PStF latency in which a second peak follows the early peak by 6–10 ms for most muscle groups tested. It is unlikely to be due to effects produced separately from each of the twin pulses because the inter-stimulus interval was 3 ms, not 6–10 ms, and given the duration of motor unit potentials with our EMG electrodes (3–5 ms), effects from the first and second pulses would tend to merge. StTA records of both ipsilateral and contralateral hindlimb PStF also typically show 2 peaks (Fig. 2) with timing similar to the time difference separating the peaks in the latency histograms in Figure 7. In some cases, the long latency PStF peak occurred without the first peak (Fig. 2, ipsilateral, FDL, SOLd). These effects could have contributed to the bimodality in the latency histograms of Figure 7. Bimodality was more common with double pulse than single-pulse stimulation although some single-pulse latency histograms show weak bimodality (Fig. 6, Monkey M, knee muscles, Monkey L, ipsilateral ankle muscles). Note that if both peaks were present in the StTA, we only measured the shortest latency peak. The mechanism of the long latency PStF effects in hindlimb muscles is unknown but presumably it

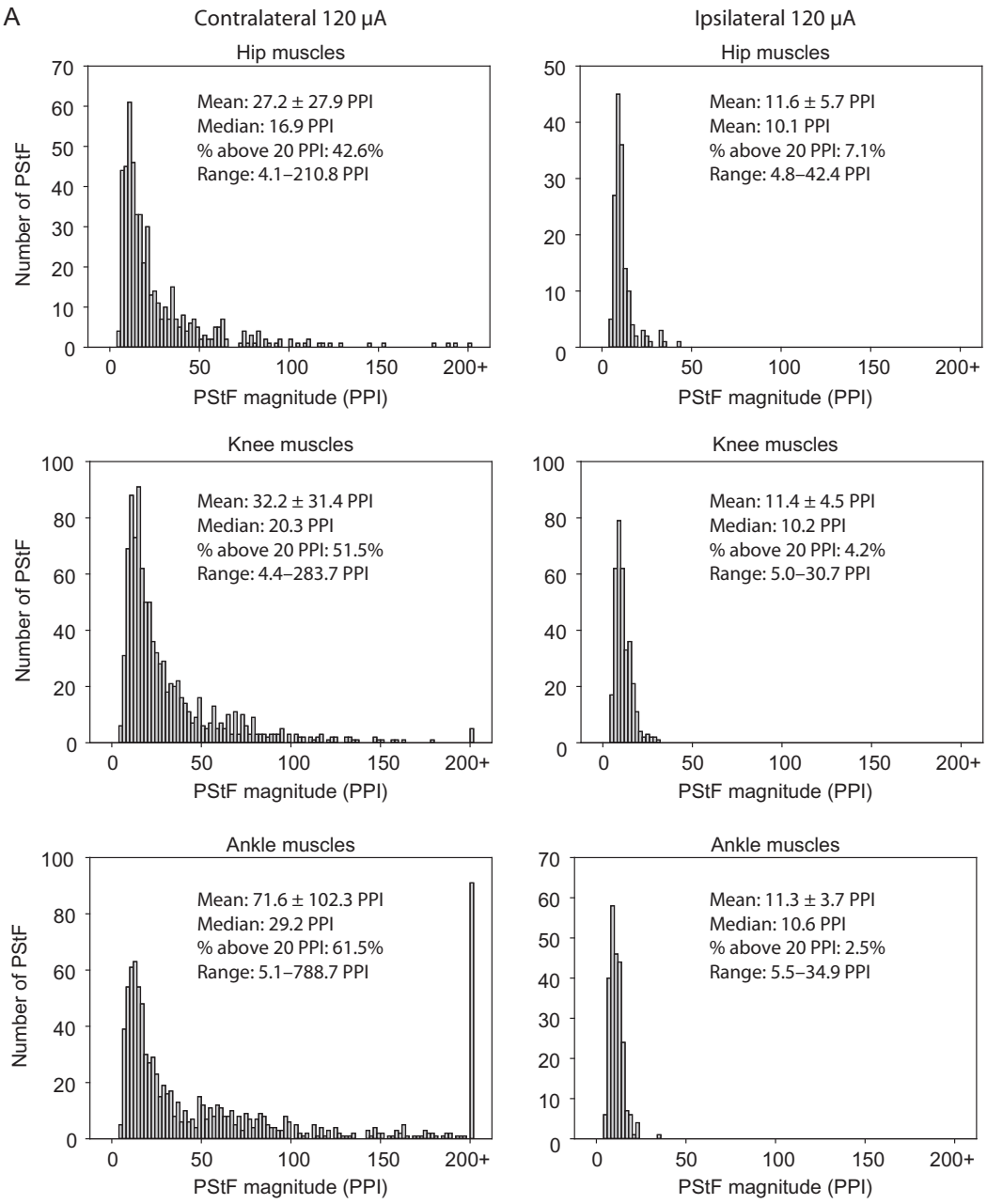

Figure 5. Distribution of PStF magnitudes for muscles at the hip, knee, ankle, digit, intrinsic foot, and all muscles combined using 120 μA stimulation of the contralateral and ipsilateral hemispheres. Data from Monkeys M and L were pooled. The mean, median, percent of effects above 20 PPI, and range for each muscle group are given. (*A*) Plots for the hip, knee, and ankle muscles. (*B*) Plots for the digit, intrinsic foot, and all muscles combined.

involves a less direct and/or slower conducting pathway to motoneurons than that mediating the short latency peak.

Compared with single-pulse stimulation, the mean onset latency of ipsilateral PStF with twin-pulse stimulation across all muscles was slightly longer in both monkeys (Table 3: 17.1 vs. 14.7 ms in Monkey L; 13.6 ms vs. 12.3 ms in Monkey M). A similar difference was observed for PStS (Table 3). The longer average latency of effects from double-pulse stimulation might be attributable to activation of less direct neural linkages requiring facilitation from 2 stimulus pulses.

Latency of PStS Effects

Figure 8 contains histograms of PStS onset latencies for all contralateral and ipsilateral muscles in each monkey at the same stimulus intensity of 120 μA. Much like PStF onset latencies, the minimum onset latencies of ipsilateral and contralateral PStS were very similar and, in fact, in Monkey L, the mean latency was slightly shorter for ipsilateral compared with contralateral effects. The mean and median values of ipsilateral and contralateral PStS were very similar and not statistically different.

Discussion

Our approach to finding the optimal stimulus parameters for detecting poststimulus effects (PStE) in muscles from microstimuli applied to the ipsilateral cortex parallels the work done in a previous study of contralateral hindlimb which determined the

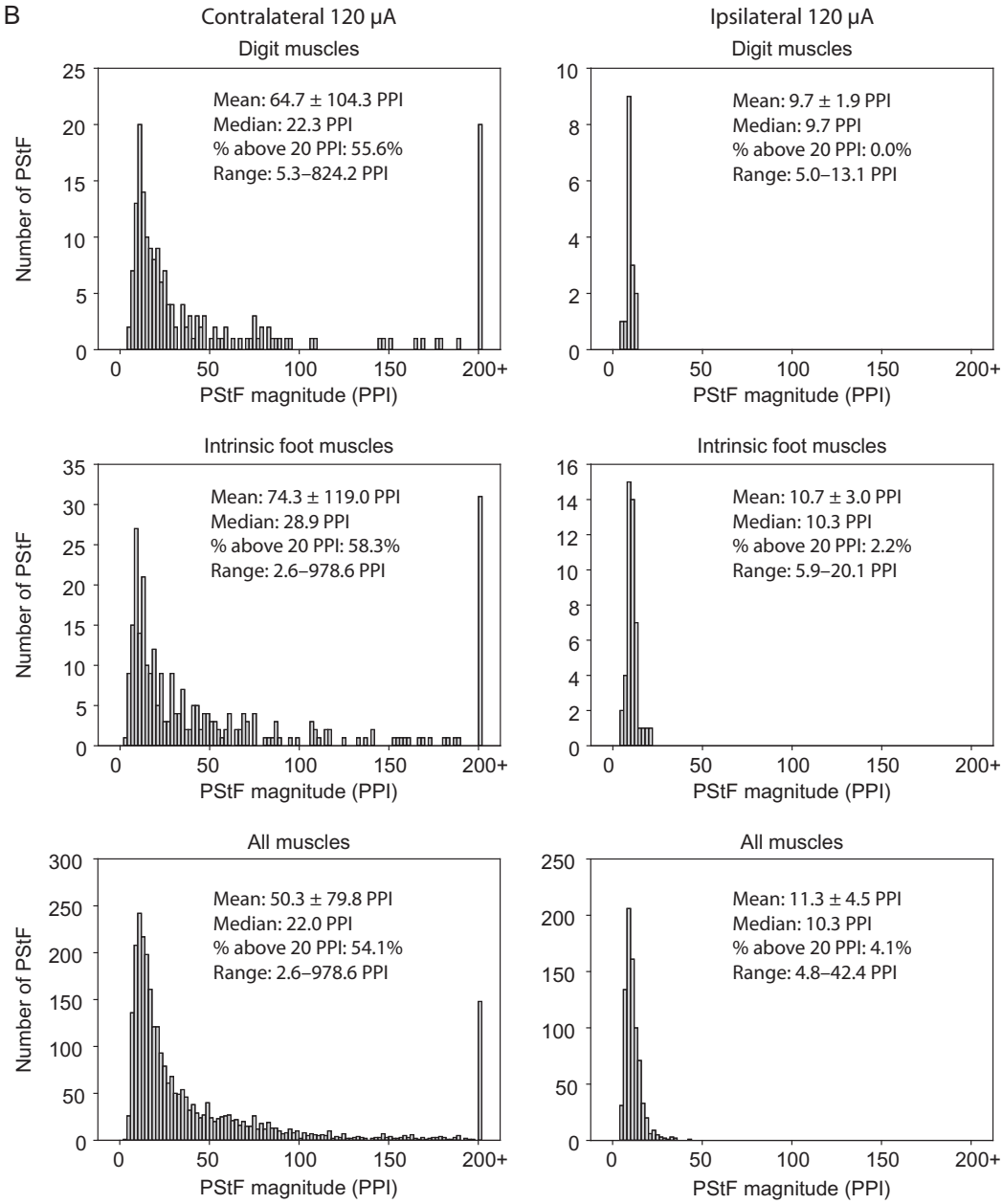

Figure 5 Continued

optimal stimulus parameters for comparison with forelimb post-stimulus effects (Hudson et al. 2015). Ipsilateral PStEs were absent at 30 μA, and there were relatively few at 60 μA—intensities yielding clear and consistent effects in contralateral M1 (Hudson et al. 2015). This was expected since we were activating a smaller population of corticospinal cells in which only 10% have been shown to descend ipsilaterally in the spinal cord (Dum and Strick 1996). To generate an adequate number of ipsilateral effects for comparison with contralateral effects, we increased the stimulus intensity to 120 μA and also used double stimulus pulses of 120 μA separated by 3 ms (twin-pulse stimulation). Our data set contains 983 PStEs ipsilaterally for comparison with 3509 PStEs contralaterally. In conclusion, these stimulus parameters provided reliable motor output effects from ipsilateral cortex that could be quantified and compared with those from contralateral cortex obtained under the same conditions.

Our results are significant in showing for the first time the existence of clear and quantifiable PStF and PStS in hindlimb muscles from ipsilateral cortex in a primate. Nevertheless, as expected, contralateral PStF was considerably stronger than ipsilateral PStF (2–6-fold) depending on the monkey and the muscle group. However, given the fact that only 10% of pyramidal axons descend in the spinal cord ipsilaterally and even some of these may cross at the spinal level, the strength of ipsilateral PStF relative to contralateral PStF (at 120 μA) might be considered surprising. Overall, contralateral PStF was 5.6 times greater than ipsilateral PStF in one monkey and 2.4 times greater in the second monkey. Contralateral PStS was less different in magnitude than ipsilateral PStS—1.8-fold greater in one monkey and 1.7 in the second monkey. The magnitudes of ipsilateral PStF were very similar in the 2 monkeys as were the magnitudes of ipsilateral PStS. However, in one monkey, the overall magnitude of contralateral

PStF was substantially greater (2.6-fold) than that in the second monkey, and this disparity was present for all muscle groups. While interesting, the reason for this difference is not clear although a similar difference was also observed in a previous study with different monkeys (Hudson et al. 2015). It is unlikely that it can be attributed to any difference in the way the monkeys

Table 3 Comparison of onset latencies of contralateral and ipsilateral PStEs

	Onset latency, ms							Onset latency, ms						
	Contralateral 120 μA		Ipsilateral 120 μA		Ipsi 2 pulse 120 μA			Contralateral 120 μA		Ipsilateral 120 μA		Ipsi 2 pulse 120 μA		
Joint	*n*	Mean ± SD	*n*	Mean ± SD	*n*	Mean ± SD	Joint	*n*	Mean ± SD	*n*	Mean ± SD	*n*	Mean ± SD	
Monkey L							Monkey M							
PStF														
Hip	299	11.8 ± 2.3	162	14.2 ± 7.2	218	13.5 ± 4.8	Hip	227	12.1 ± 3.5	81	15.7 ± 6.2	138	15.9 ± 5.4	
Knee	707	12.1 ± 3.6	320	15.5 ± 6.8	541	15.8 ± 5.0	Knee	539	11.7 ± 3.6	312	12.1 ± 4.1	466	13.8 ± 4.5	
Ankle	656	13.3 ± 2.1	115	17.5 ± 6.4	300	18.7 ± 5.0	Ankle	414	12.8 ± 2.1	94	14.0 ± 5.8	279	12.8 ± 3.8	
Digit	129	13.7 ± 3.3	38	22.3 ± 7.7	54	19.5 ± 6.6	Digit	96	13.6 ± 1.7	25	15.0 ± 4.9	56	14.2 ± 4.1	
Intrinsic	384	13.7 ± 3.9	192	14.1 ± 5.7	371	16.3 ± 6.5	Intrinsic	229	14.3 ± 2.8	110	12.8 ± 4.7	168	15.0 ± 4.7	
Total	2175	12.8 ± 3.2	827	15.5 ± 6.9	1484	16.3 ± 5.7	Total	1505	12.6 ± 3.2	622	13.1 ± 5.0	1107	14.0 ± 4.6	
PStS														
Hip	116	14.9 ± 3.7	75	15.9 ± 5.7	148	16.2 ± 3.7	Hip	108	22.2 ± 9.2	38	22.3 ± 10.1	80	20.4 ± 6.3	
Knee	125	16.3 ± 3.9	91	17.3 ± 5.6	202	17.3 ± 3.9	Knee	177	18.4 ± 6.2	68	19.1 ± 7.8	101	20.4 ± 8.7	
Ankle	39	19.6 ± 4.0	45	17.9 ± 4.1	73	22.6 ± 7.0	Ankle	85	19.7 ± 8.0	34	19.3 ± 4.0	95	23.1 ± 7.0	
Digit	18	18.5 ± 4.8	20	19.4 ± 6.3	62	20.1 ± 5.0	Digit	12	19.7 ± 8.0	4	14.5 ± 4.2	5	18.2 ± 1.4	
Intrinsic	26	20.8 ± 5.6	18	22.2 ± 10.3	13	31.3 ± 10.6	Intrinsic	52	23.7 ± 6.5	10	21.3 ± 5.5	16	29.2 ± 7.9	
Total	324	16.7 ± 4.5	249	17.5 ± 6.1	498	18.5 ± 5.7	Total	434	20.6 ± 7.5	154	20.0 ± 7.8	297	21.7 ± 7.8	

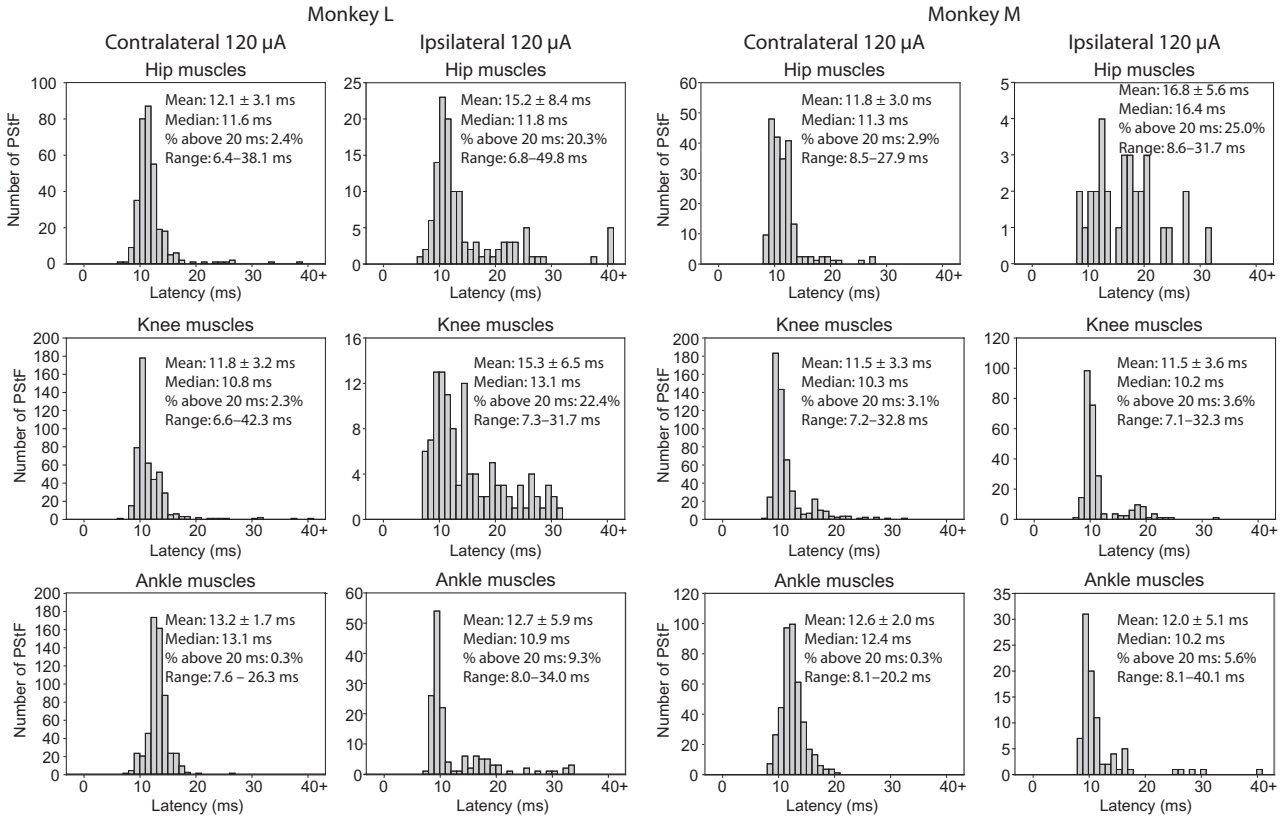

Figure 6. Distribution of PStF onset latencies for muscles at the hip, knee, ankle, digit, and intrinsic foot muscles using 120 μA stimulation in the contralateral and ipsilateral hemispheres of Monkey M and Monkey L. The mean, median, percent of latencies longer than 20 ms, and range for each muscle group are given. (*A*) Plots for hip, knee, and ankle muscles. (*B*) Plots for digit, intrinsic foot, and all muscles.

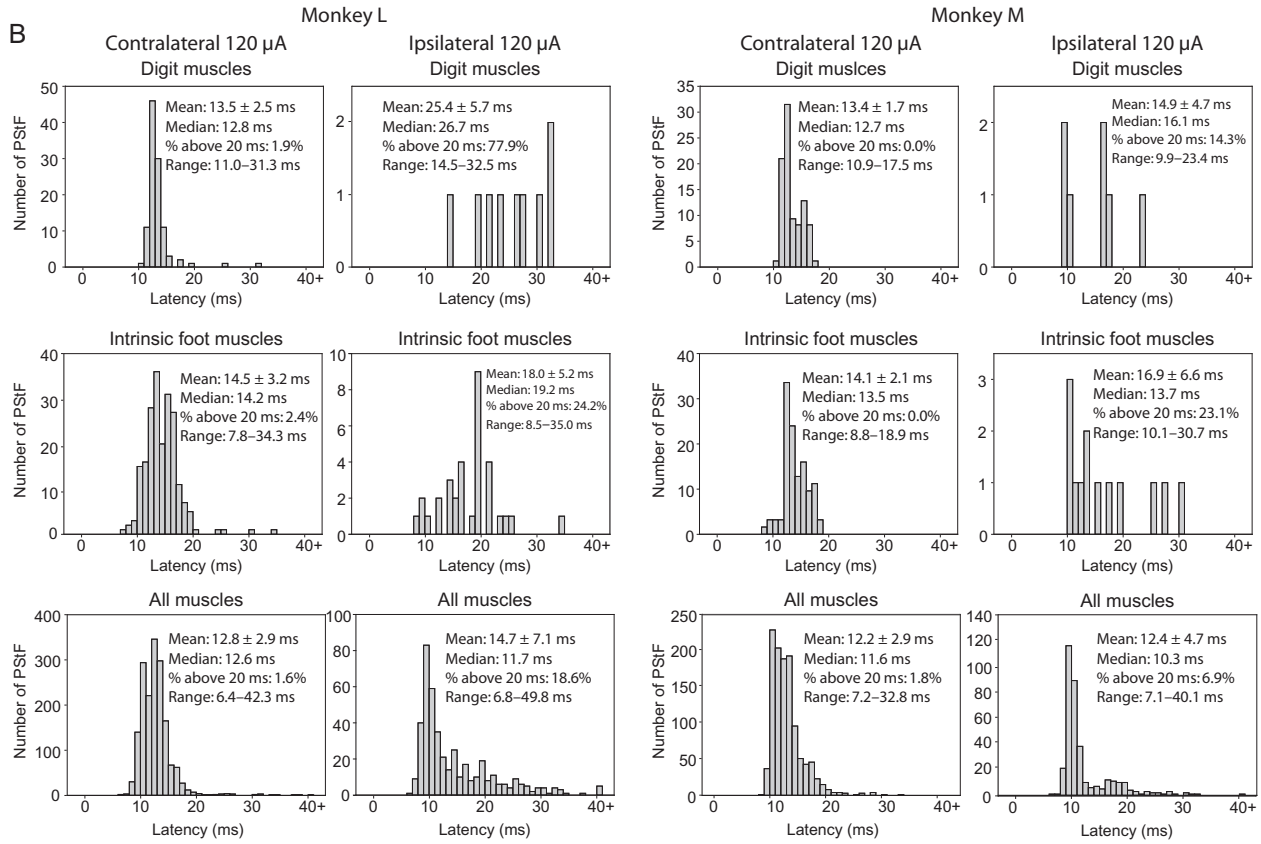

Figure 6 Continued

performed the task or the overall level of EMG activity. We measured the task-related level of EMG activation across all muscles for the EMG implants in the 2 monkeys and found there was no significant difference (0.0992 ± 0.523 and 0.1036 ± 0.0511, arbitrary units, $P = 0.5539$). We have not observed this level of PStF magnitude disparity across subjects in studies of cortical output to forelimb muscles (Park et al. 2004). These inter-subject differences presumably correlate with differences in some aspect of the synaptic linkage with motoneurons between the 2 monkeys.

The latency of effects in stimulus-triggered averages provides insight as to the directness of the synaptic linkage underlying PStF and PStS. Most noteworthy is the fact that the shortest onset latency ipsilateral PStF was as short (difference of 0.4 ms or less) as the shortest latency contralateral PStF in 5 of 6 muscle group comparisons (hip, knee, and ankle muscles in both monkeys). Distal and intrinsic foot muscle groups had too few ipsilateral effects to be confident of the shortest latency effect. These results suggest that in many cases the combination of synaptic linkage and conduction velocity of the neurons in the pathway from cortex to muscle are equally as fast for ipsilateral PStF as contralateral PStF. We assume that in macaque monkeys, the conduction velocity of ipsilateral corticospinal neurons might be similar to contralateral projecting corticospinal neurons, although there is evidence in humans age 4 and older that ipsilateral conduction velocity is only about half that of contralaterally projecting neurons (Eyre 2003). In any case, it is highly unlikely that the conduction velocity of the neurons in the ipsilateral pathway would actually be faster than the contralateral pathway. Accordingly, we conclude that the minimum synaptic linkage for ipsilateral PStF is likely to be the same as for contralateral PStF and that it is probably monosynaptic (Jankowska et al. 1975). This conclusion is supported by the results of BDA labeled and reconstructed single corticospinal axons terminating ipsilaterally in lamina IX of the spinal cord with boutons in close apposition to motoneurons (Lacroix et al. 2004). Nevertheless, while the shortest latency effects might be monosynaptic both contralaterally and ipsilaterally, it is important to emphasize that the densest corticospinal terminations are to spinal lamina outside the motoneuron pools (Dum and Strick 1996). The fact that a large fraction of not only the ipsilateral PStF effects but also the contralateral effects have latencies much greater than the shortest latency effects is consistent with the anatomical data showing the densest corticospinal terminations in the intermediate lamina of the spinal cord.

While the ipsilateral corticospinal projection is an obvious source of ipsilateral effects, other potential neural circuits cannot be ruled out. Other circuits would include 1) crossed corticospinal axons that synapse on spinal interneurons that then re-cross the midline at the segmental level, 2) cortico-cortical trans-callosal axons that synapse with contralateral corticospinal neurons (Matsunami and Hamada 1984), and 3) cortico-bulbar pathways, particularly to reticulospinal neurons (Edgley et al. 2004; Davidson and Buford 2006; Schepens and Drew 2006; Davidson et al. 2007; Jankowska and Stecina 2007; Stecina and Jankowska 2007; Baker 2011).

Soteropoulos et al. (2011) investigated ipsilateral corticospinal contributions to forelimb muscles in the rhesus macaque using a variety of approaches including intracellular recording from motoneurons, stimulus-triggered averaging of EMG activity, spike-triggered averaging of EMG activity, strong stimulation of

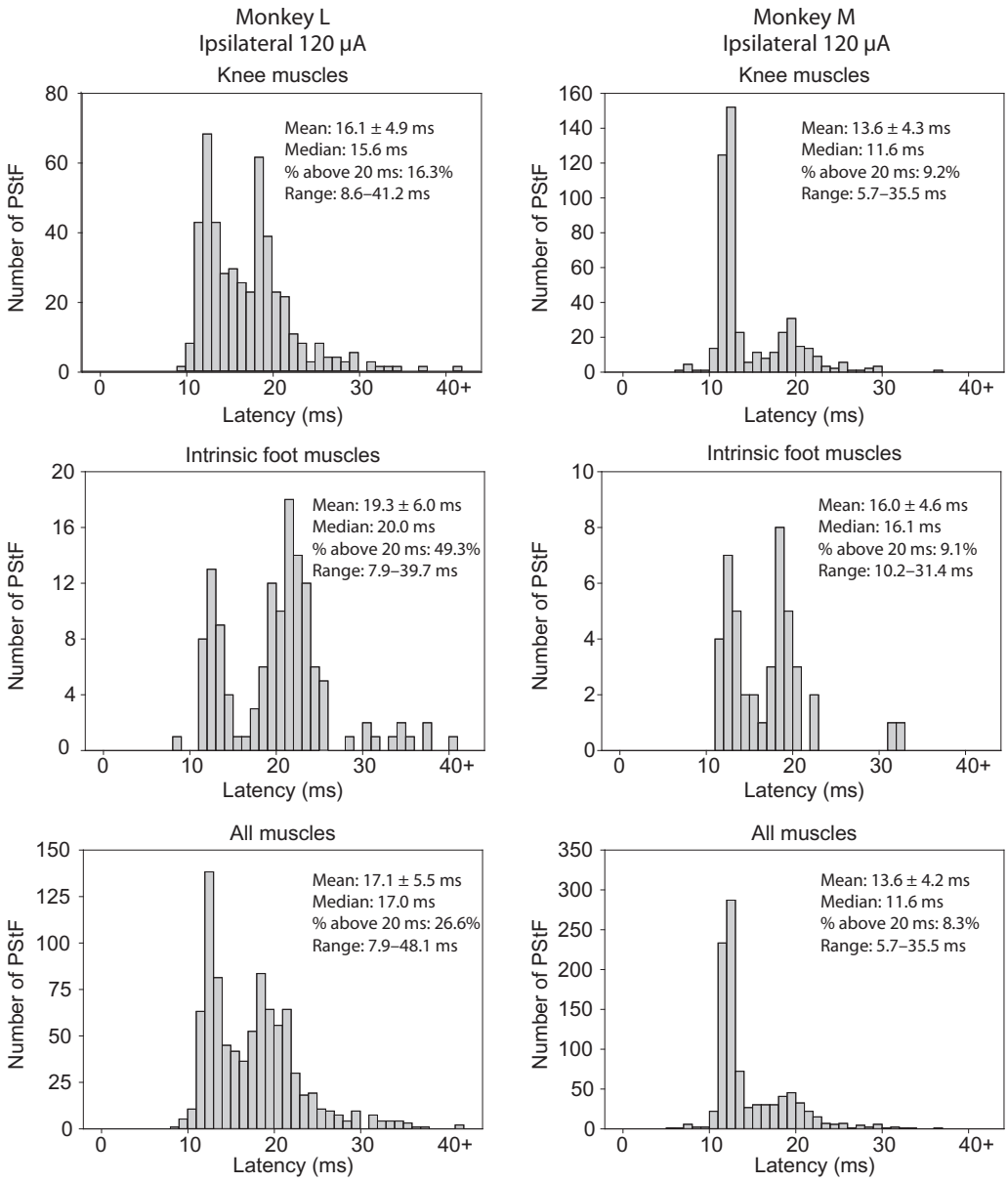

Figure 7. Distribution of ipsilateral PStF onset latencies for twin-pulse stimulation at 120 μA. Shown are a proximal muscle group (knee), a distal muscle group (intrinsic foot), and all muscles (hip, knee, ankle, digit, and intrinsic foot) combined for Monkeys L and M. Individual stimuli comprising the twin pulse were separated by 3 ms and repeated at a frequency of 5 Hz. The mean, median, percent of latencies longer than 20 ms, and range for each muscle group are also given.

corticospinal axons in the medullary pyramids, and cortical unit activity in relation to a reach and precision grip task. Intracellular recordings revealed no monosynaptic EPSPs after stimulating the ipsilateral pyramidal tract, and only a few weak oligosynaptic EPSPs were observed. Spike-triggered averaging of EMG activity revealed significant effects in ipsilateral muscles, but all of them were rejected based on an onset latency that was too early or a peak that was too broad to be consistent with a monosynaptic linkage. Similarly, stimulus-triggered averaging from ipsilateral cortex revealed no genuine effects at intensities up to 30 μA.

In contrast to the work of Soteropoulos et al. (2011) on forelimb M1 cortex, we did find consistent and significant effects from M1 on ipsilateral hindlimb muscles with stimulus-triggered averaging of EMG activity. In addition to forelimb versus hindlimb, another important difference between our study and that of Soteropoulos was that we used substantially higher stimulus intensities (120 vs. 30 μA). In fact, at 30 μA, our results are completely consistent with those of Soteropoulos et al. (2011) in that we found no ipsilateral PStEs at 30 μA that met our acceptance criteria. Even at 60 μA, the effects were relatively scarce and very weak (Fig. 2). However, at 120 μA, clear and prevalent PStEs were obtained and formed an excellent basis for comparison with contralateral PStEs at the same intensity. Another difference between our study and Soteropoulos is that we systematically explored the full extent of the M1 representation and tested many more cortical sites (314 vs. 27). Nevertheless, given the impressive use of different approaches, including stimulation of the pyramidal tract coupled with averaging intracellular responses, it is puzzling why not more than 2 of 62 motoneurons tested showed effects. Based on the results of the current study, more effects might have been expected. This raises

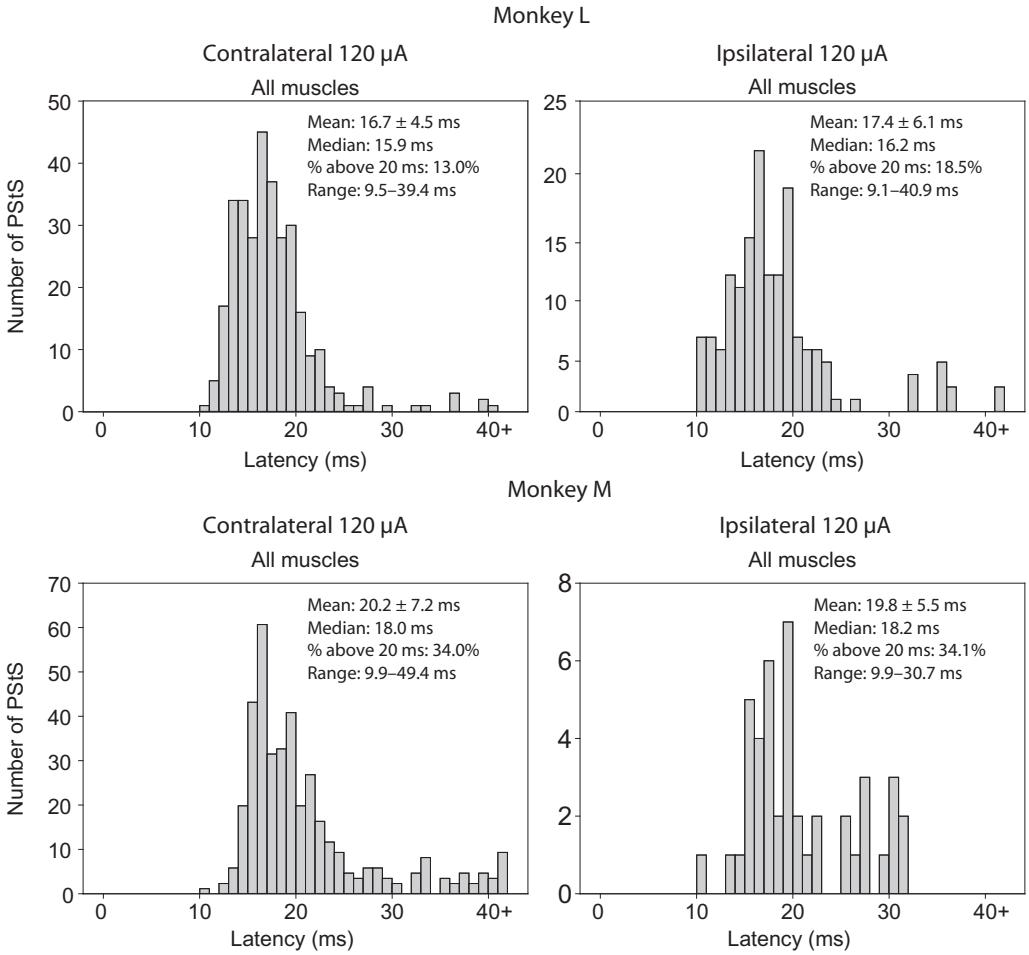

Figure 8. Distribution of PStS onset latencies for all muscles combined using 120 µA single-pulse stimulus triggered averaging from sites in the contralateral and ipsilateral hemispheres of Monkey M and Monkey L. The mean, median, percent of latencies longer than 20 ms, and range for each muscle group are given.

the real possibility of a genuine difference in organization of forelimb and hindlimb corticospinal projections. As stated earlier, neuroanatomical evidence supports the existence of ipsilateral monosynaptic linkages from corticospinal neurons to hindlimb motoneurons (Lacroix et al. 2004).

Why do ipsilateral effects require relatively high stimulus intensities to be revealed with stimulus-triggered averaging? The fact that only 10% of corticospinal neurons descend ipsilaterally means the density of ipsilaterally projecting neurons in the cortex will be relatively sparse. What stimulus intensity would activate a similar number of contralaterally projecting cells as the number of ipsilaterally projecting cells activated at 120 µA? Based on the equation $r^2 = i/k$, where r is the radius of excited cells in millimeters, i is the stimulus current in microamperes and k is an intermediate proportionality constant (1350 µA/mm^2), the expected radius for physical spread of excitatory current at 120 µA would be ~0.3 mm (Cheney and Fetz 1985). Using a density of 288 corticospinal neurons/mm^2 (Cheney et al. 2000) yields 271 neurons activated by a current of 120 µA. Assuming that only 27 of these neurons project ipsilaterally (10%), we can ask what current would be required to activate 27 contralaterally projecting neurons? Using the density of corticospinal neurons and the equation above yields a current of 45 µA to activate 27 contralaterally projecting corticospinal neurons. Extrapolating from stimulus-triggered averaging results for contralateral hindlimb muscles at 30 and 60 µA (Hudson et al. 2013), 45 µA would produce a mean PStF magnitude of 35.6 PPI. In fact, a current of 120 µA, which should activate ~27 ipsilaterally projecting cells, actually produced a PStF magnitude in ipsilateral muscles of 11.3 PPI. Accordingly, the difference in the magnitude of contralateral and ipsilateral PStF (35.6 vs. 11.3 PPI) seems unlikely to be explained simply based on differences in the expected number of contralaterally and ipsilaterally projecting corticospinal neurons. Rather, the results suggest a substantially weaker overall synaptic linkage, either due to weaker synapses or a predominantly less direct synaptic linkage. A predominantly less direct synaptic linkage would be consistent with the finding that the overall mean onset latency of PStF for most muscle groups in both monkeys was significantly greater for ipsilateral PStF.

A final issue deserves mention. Is there any possibility that our stimulus current could have spread to the contralateral cortex? Again, based on the equation mentioned earlier, a current of 120 µA would be expected to excite corticospinal cells in a sphere with a radius of 0.3 mm. Even the closest electrode tracts to the contralateral cortex (Fig. 3) were >3 mm away so there is little or no possibility of physical current spread to the contralateral hemisphere. Of course, most stimulus sites in ipsilateral cortex were much further away than 3 mm from the contralateral cortex.

Funding

This work was supported by NIH Grants NS051825 (PDC), NS064054 (PDC), NIH Center Grant HD02528, T32HD057850 training grant (WGM) and the Kathleen M. Osborn Endowment.

Notes

The authors thank Ian Edwards for technical assistance. *Conflict of Interest*: None declared.

References

Aizawa H, Mushiake H, Inase M, Tanji J. 1990. An output zone of the monkey primary motor cortex specialized for bilateral hand movement. Exp Brain Res. 82:219–221.

Baker SN. 2011. The primate reticulospinal tract, hand function and functional recovery. J Physiol. 589:5603–5612.

Benecke R, Meyer BU, Freund HJ. 1991. Reorganisation of descending motor pathways in patients after hemispherectomy and severe hemispheric lesions demonstrated by magnetic brain stimulation. Exp Brain Res. 83:419–426.

Boudrias MH, Belhaj-Saif A, Park MC, Cheney PD. 2006. Contrasting properties of motor output from the supplementary motor area and primary motor cortex in rhesus macaques. Cereb Cortex. 16:632–638.

Brus-Ramer M, Carmel JB, Chakrabarty S, Martin JH. 2007. Electrical stimulation of spared corticospinal axons augments connections with ipsilateral spinal motor circuits after injury. J Neurosci. 27:13793–13801.

Caramia MD, Palmieri MG, Giacomini P, Iani C, Dally L, Silvestrini M. 2000. Ipsilateral activation of the unaffected motor cortex in patients with hemiparetic stroke. Clin Neurophysiol. 111:1990–1996.

Cheney PD, Fetz EE. 1985. Comparable patterns of muscle facilitation evoked by individual corticomotoneuronal (CM) cells and by single intracortical microstimuli in primates: evidence for functional groups of CM cells. J Neurophysiol. 53:786–804.

Cheney PD, Fetz EE, Palmer SS. 1985. Patterns of facilitation and suppression of antagonist forelimb muscles from motor cortex sites in the awake monkey. J Neurophysiol. 53:805–820.

Cheney PD, Hill-Karrer J, Belhaj-Saif A, McKiernan BJ, Park MC, Marcario JK. 2000. Cortical motor areas and their properties: implications for neuroprosthetics. Prog Brain Res. 128:135–160.

Chiou SY, Wang RY, Liao KK, Wu YT, Lu CF, Yang YR. 2013. Co-activation of primary motor cortex ipsilateral to muscles contracting in a unilateral motor task. Clin Neurophysiol. 124:1353–1363.

Chollet F, DiPiero V, Wise RJ, Brooks DJ, Dolan RJ, Frackowiak RS. 1991. The functional anatomy of motor recovery after stroke in humans: a study with positron emission tomography. Ann Neurol. 29:63–71.

Cramer SC, Finklestein SP, Schaechter JD, Bush G, Rosen BR. 1999. Activation of distinct motor cortex regions during ipsilateral and contralateral finger movements. J Neurophysiol. 81:383–387.

Curt A, Alkadhi H, Crelier GR, Boendermaker SH, Hepp-Reymond MC, Kollias SS. 2002. Changes of non-affected upper limb cortical representation in paraplegic patients as assessed by fMRI. Brain. 125:2567–2578.

Davidson AG, Buford JA. 2006. Bilateral actions of the reticulospinal tract on arm and shoulder muscles in the monkey: stimulus triggered averaging. Exp Brain Res. 173:25–39.

Davidson AG, Buford JA. 2004. Motor outputs from the primate reticular formation to shoulder muscles as revealed by stimulus-triggered averaging. J Neurophysiol. 92:83–95.

Davidson AG, Schieber MH, Buford JA. 2007. Bilateral spike-triggered average effects in arm and shoulder muscles from the monkey pontomedullary reticular formation. J Neurosci. 27:8053–8058.

Dum RP, Strick PL. 1996. Spinal cord terminations of the medial wall motor areas in macaque monkeys. J Neurosci. 16:6513–6525.

Edgley SA, Jankowska E, Hammar I. 2004. Ipsilateral actions of feline corticospinal tract neurons on limb motoneurons. J Neurosci. 24:7804–7813.

Eyre JA. 2003. Development and plasticity of the corticospinal system in man. Neural Plast. 10:93–106.

Feydy A, Carlier R, Roby-Brami A, Bussel B, Cazalis F, Pierot L, Burnod Y, Maier MA. 2002. Longitudinal study of motor recovery after stroke: recruitment and focusing of brain activation. Stroke. 33:1610–1617.

Fisher CM. 1992. Concerning the mechanism of recovery in stroke hemiplegia. Can J Neurol Sci. 19:57–63.

Gharbawie OA, Karl JM, Whishaw IQ. 2007. Recovery of skilled reaching following motor cortex stroke: do residual corticofugal fibers mediate compensatory recovery? Eur J Neurosci. 26:3309–3327.

Griffin DM, Hudson HM, Belhaj-Saif A, Cheney PD. 2009. Stability of output effects from motor cortex to forelimb muscles in primates. J Neurosci. 29:1915–1927.

He XW, Wu CP. 1985. Connections between pericruciate cortex and the medullary reticulospinal neurons in cat: an electrophysiological study. Exp Brain Res. 61:109–116.

Hudson HM, Griffin DM, Belhaj-Saif A, Cheney PD. 2013. Cortical output to fast and slow muscles of the ankle in the rhesus macaque. Front Neural Circuits. 7:33.

Hudson HM, Griffin DM, Belhaj-Saif A, Cheney PD. 2015. Properties of primary motor cortex output to hindlimb muscles in the macaque monkey. J Neurophysiol. 113:937–949.

Hudson HM, Griffin DM, Belhaj-Saif A, Lee SP, Cheney PD. 2010. Methods for chronic recording of EMG activity from large numbers of hindlimb muscles in awake rhesus macaques. J Neurosci Methods. 189:153–161.

Hutchins KD, Martino AM, Strick PL. 1988. Corticospinal projections from the medial wall of the hemisphere. Exp Brain Res. 71:667–672.

Jankowska E, Edgley SA. 2006. How can corticospinal tract neurons contribute to ipsilateral movements? A question with implications for recovery of motor functions. Neuroscientist. 12:67–79.

Jankowska E, Padel Y, Tanaka R. 1975. Projections of pyramidal tract cells to alpha-motoneurones innervating hind-limb muscles in the monkey. J Physiol. 249:637–667.

Jankowska E, Stecina K. 2007. Uncrossed actions of feline corticospinal tract neurones on lumbar interneurones evoked via ipsilaterally descending pathways. J Physiol. 580:133–147.

Kasser RJ, Cheney PD. 1985. Characteristics of corticomotoneuronal postspike facilitation and reciprocal suppression of EMG activity in the monkey. J Neurophysiol. 53:959–978.

Keizer K, Kuypers HG. 1989. Distribution of corticospinal neurons with collaterals to the lower brain stem reticular formation in monkey (*Macaca fascicularis*). Exp Brain Res. 74:311–318.

Lacroix S, Havton LA, McKay H, Yang H, Brant A, Roberts J, Tuszynski MH. 2004. Bilateral corticospinal projections arise from each motor cortex in the macaque monkey: a quantitative study. J Comp Neurol. 473:147–161.

Luppino G, Matelli M, Camarda RM, Gallese V, Rizzolatti G. 1991. Multiple representations of body movements in mesial area 6 and the adjacent cingulate cortex: an intracortical microstimulation study in the macaque monkey. J Comp Neurol. 311:463–482.

Macpherson JM, Marangoz C, Miles TS, Wiesendanger M. 1982. Microstimulation of the supplementary motor area (SMA) in the awake monkey. Exp Brain Res. 45:410–416.

Matsunami K, Hamada I. 1984. Effects of stimulation of corpus callosum on precentral neuron activity in the awake monkey. J Neurophysiol. 52:676–691.

Matsunami K, Hamada I. 1978. Precentral neuron activity associated with ipsilateral forelimb movements in monkeys. J Physiol (Paris). 74:319–322.

Mitz AR, Wise SP. 1987. The somatotopic organization of the supplementary motor area: intracortical microstimulation mapping. J Neurosci. 7:1010–1021.

Palmer E, Ashby P, Hajek VE. 1992. Ipsilateral fast corticospinal pathways do not account for recovery in stroke. Ann Neurol. 32:519–525.

Park MC, Belhaj-Saif A, Cheney PD. 2000. Chronic recording of EMG activity from large numbers of forelimb muscles in awake macaque monkeys. J Neurosci Methods. 96:153–160.

Park MC, Belhaj-Saif A, Cheney PD. 2004. Properties of primary motor cortex output to forelimb muscles in rhesus macaques. J Neurophysiol. 92:2968–2984.

Park MC, Belhaj-Saif A, Gordon M, Cheney PD. 2001. Consistent features in the forelimb representation of primary motor cortex in rhesus macaques. J Neurosci. 21:2784–2792.

Riddle CN, Edgley SA, Baker SN. 2009. Direct and indirect connections with upper limb motoneurons from the primate reticulospinal tract. J Neurosci. 29:4993–4999.

Schepens B, Drew T. 2006. Descending signals from the pontomedullary reticular formation are bilateral, asymmetric, and gated during reaching movements in the cat. J Neurophysiol. 96:2229–2252.

Snider RS, Lee JC. 1961. A Stereotaxic Atlas of the Monkey Brain (*Macaca mulatta*). Chicago: University of Chicago Press.

Soteropoulos DS, Edgley SA, Baker SN. 2011. Lack of evidence for direct corticospinal contributions to control of the ipsilateral forelimb in monkey. J Neurosci. 31:11208–11219.

Stecina K, Jankowska E. 2007. Uncrossed actions of feline corticospinal tract neurones on hindlimb motoneurones evoked via ipsilaterally descending pathways. J Physiol. 580:119–132.

Tanji J, Okano K, Sato KC. 1988. Neuronal activity in cortical motor areas related to ipsilateral, contralateral, and bilateral digit movements of the monkey. J Neurophysiol. 60:325–343.

Verstynen T, Diedrichsen J, Albert N, Aparicio P, Ivry RB. 2005. Ipsilateral motor cortex activity during unimanual hand movements relates to task complexity. J Neurophysiol. 93:1209–1222.